Roughness effect on the measurement of interface stress

Palasantzas, G.; de Hosson, J.T.M.

Published in:
Acta Materialia

DOI:
10.1016/S1359-6454(00)00170-1

Publication date:
2000

Pergamon

Acta mater. 48 (2000) 3641–3645

Acta MATERIALIA

www.elsevier.com/locate/actamat

ROUGHNESS EFFECT ON THE MEASUREMENT OF INTERFACE STRESS

G. PALASANTZAS and J. Th. M. DE HOSSON*

Department of Applied Physics, Materials Science Center and Netherlands Institute for Metals Research, University of Groningen, Nijenborgh 4, 9747 AG, Groningen, The Netherlands

(Received 3 April 2000; received in revised form 30 May 2000; accepted 30 May 2000)

Abstract—Stimulated by a recent paper by Spaepen (Acta mater. 48 (2000) 31) we concentrate on the effect of roughness parameters on stress measurements in thin films for self-affine and mound rough interfaces. A self-affine interface is characterized by a lateral correlation length ξ, an rms roughness amplitude σ, and a roughness exponent H ($0 < H < 1$). With increasing long wavelength roughness ratio σ/ξ, the ratio between the measured and the actual interface stress decreases. It decreases with a decreasing roughness exponent H that leads to rougher interfaces at short roughness wavelengths ($< \xi$). For mound roughness which is characterised besides σ by an average mound separation λ and a system correlation length ζ, the force ratio decays in an oscillatory manner as a function of σ/λ as long as $\lambda < \zeta$. It is concluded that for both cases a more precise knowledge of roughness morphology is required in order to address the influence of interface roughness on the interface stress in thin films. *© 2000 Acta Metallurgica Inc. Published by Elsevier Science Ltd. All rights reserved.*

Keywords: Mesostructure; Thin films; Interfaces; Grain boundaries; Stress

1. INTRODUCTION

Intrinsic stress developments in thin monocrystalline films are not caused by differential thermal expansion between the film and the substrate, or by directly applied external loads. A classic example is the epitaxial growth of films of single crystals where the structure and to some extent the energetic of semicoherent interfaces are known from experimental observations and (dislocation) theory [1, 2]. On the other hand, for polycrystalline films various mechanisms have been proposed to explain the accumulation of stresses. The grain boundaries in these films may contribute to a densification by acting as sinks for excess vacancies, or by eliminating excess boundary volume as a result of grain growth [3]. The competition between surface and grain boundary energies may force the coalescence of crystallites and generate tensile stresses [4–7]. Grain boundaries can also play a role in the relaxation of stresses by plastic flow, either as obstacles to dislocation motion or as sources and sinks in diffusional flow [7].

In many cases, the growth front of the film can be rough because steps and ledges are formed during growth of a multi-layer [8–11]. Also, noise-induced roughening may lead to the formation of self-affine fractal morphologies [12–15]. In the former case the existence of an asymmetric step–edge diffusion barrier, or Schwoebel barrier, inhibits the down-hill diffusion of incoming atoms leading effectively to the creation of large structures in the form of mounds (unstable growth) [8–11]. Different interface morphology in multi-layer films would possibly lead to distinct stress contributions. Under certain circumstances the fractality can be investigated by local probe techniques [16, 17].

Indeed, as was shown by Spaepen [7], interface roughness can lower the measured stress in a manner that strongly depends on the particular interface morphology. In his work [7], an application was performed for sinusoidal roughness where it was shown that with increasing ratio of oscillation amplitude over oscillation wavelength (rougher interface), a substantial decrement of approximately 60% was obtained for ratios near unity. However, it was pointed out that in many cases such a variation would be much smaller [7].

Stimulated by Spaepen's work we have extended his approach to the more general cases of random self-affine and mound rough interfaces, which are commonly observed during multi-layer growth [18–21], as well as mound interface roughness that develops during epitaxial growth [8–11, 22]. Our work is in both cases executed in the weak roughness

* To whom all correspondence should be addressed.

PII: S1359-6454(00)00170-1

limit because in many cases of thin film growth the corresponding ratio of vertical, out-of-film-plane roughness amplitude to lateral, in-plane correlation length is equal or lower than 0.1 [12–15, 18–21].

2. ROUGHNESS EFFECTS ON THE MEASUREMENT OF INTERFACE STRESS

We denote the interface height profile by $h(r)$ which is assumed to be a single valued function of the in-plane position vector $r = (x,y)$. The interface area between r and $r + d^2r$ is given by $dA = [1 + (\nabla h)^2]^{1/2}$. This is similar to Spaepen but now concentrating on area instead of length. Upon stretching the interface by a small amount $\Delta\varepsilon$ in the x–y plane, assuming all positions shift while the z-positions remain the same such that dr deforms to $dr(1 + \Delta\varepsilon)$, the area of the deformed interface changes to first order in $\Delta\varepsilon$ by $dA' = [(1 + \Delta\varepsilon)^2 + (\nabla h)^2]^{1/2} d^2r \approx [1 + (\nabla h)^2]^{1/2}\{1 + 2\Delta\varepsilon/[1 + (\nabla h)^2]\}^{1/2} d^2r$ which results in a change of interface area by $\delta A = dA' - dA \approx \{\Delta\varepsilon/[1 + (\nabla h)^2]^{1/2}\}\mathrm{d}^2r$. Thus, the work dW necessary to stretch this part of the interface area elastically is $F\delta A$ (assuming F to be isotropic) which upon integration over the entire interface yields the total work

$$W \approx F\Delta\varepsilon \int d^2r/[1 + (\nabla h)^2]^{1/2}. \tag{1}$$

This work is related to the apparent or measured interface stress by $W = F_m\Delta\varepsilon\mathrm{A}$ where A is the projected or apparent area of the interface in the x–y plane. As a result, the ratio between the measured and the actual interface stress for a planar interface is

$$F_m/F \approx (1/A) \int d^2r/[1 + (\nabla h)^2]^{1/2}. \tag{2}$$

For a weak roughness $|\nabla h| \ll 1$, and $[1 + (\nabla h)^2]^{-1/2} \approx 1 - (1/2)(\nabla h)^2 + (3/8)(\nabla h)^4 ...$ Substitution of the leading terms of this series expansion into equation (2) yields up to second order (see Appendix A)

$$F_m/F \approx 1 - \frac{1}{2}\int (\nabla h)^2 d^2r + \frac{3}{8}\int (\nabla h)^4 d^2r \tag{3}$$

where the average flat interface area is given by $A \approx \int d^2r$. Furthermore, the interface height profile $h(r)$ is assumed to be a stationary stochastic process with $\langle h(r)\rangle = 0$, and an interface isotropy along the x and y axes. In addition, we shall assume that $h(r)$ is a random Gaussian variable in order to calculate the ensemble averaged products of $h(r)$s (see Appendix A). We define the Fourier transform of $h(r)$ as $h(q) = (2\pi)^{-2}\int h(r)e^{-\mathrm{iqr}}d^2r$ and assume interfaces that are statistically stationary up to second order or transitionally invariant such that

$$\langle h(q)h(q')\rangle = \frac{(2\pi)^4}{A}\langle|h(q)|^2\rangle\delta^2(q - q'). \tag{4}$$

Thus using equations (3) and (4) and equations (A.4) and (A.5) from Appendix A, we obtain

$$F_m/F \approx 1 - \frac{1}{2}\rho^2 + \frac{9}{8}\rho^4,\ \rho = \left\{\frac{(2\pi)^4}{A}\int q^2\langle|\mathrm{h(q)}|^2\rangle d^2q\right\}^{1/2} \tag{5}$$

with $\rho(=\langle|\nabla h|^2\rangle^{1/2})$ is termed as the average interface local slope.

3. RANDOM ROUGHNESS MODEL

3.1. Self-affine roughness

The nanometer scale topology of vapor-deposited single/multi-layer thin films can be quantified in many cases in terms of self-affine roughness [12–15, 18–21]. In general, any physical self-affine surface or interface is characterized by a finite lateral correlation length ξ, an rms roughness amplitude σ, and a roughness exponent H ($0 < H < 1$) [12–15]. The roughness exponent H is a measure of the degree of interface irregularity at short roughness wavelengths ($< \xi$) such that small values of $H(\sim 0)$ characterize extremely jagged or irregular interfaces, while large values of $H(\sim 1)$ characterize interfaces with smooth hills and valleys (Fig. 1) [12–15]. With the exponent after Hurst, a hydrologist examining together with Mandelbrodt scaling properties of river fluctuations, it is assumed that the self-affine interface is fractal up

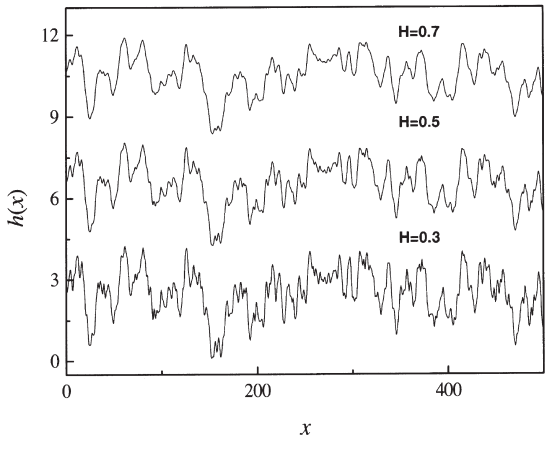

Fig. 1. Surface profiles at different values of H. These three surfaces possess the same values for σ and ξ, but different values for the roughness exponent H (axes in arbitrary units).

to a correlation length ξ. In real space the self-affine interface $h(r)$ can be considered at a point r by $h(r) = (r/\xi)^H$. However, it should be emphasized that the concept of fractal dimension is not intrinsically related to H. The fractal dimension will only be defined once the measuring tool is specified. For self-affine fractals $\langle|h(q)|^2\rangle$ is characterized by the power scaling behavior $\langle|h(q)|^2\rangle \propto q^{-2-2H}$ if $q\xi \gg 1$, and $\langle|h(q)|^2\rangle \propto$ const if $q\xi \ll 1$ [12–15]. This scaling behavior in Fourier space is satisfied by the simple Lorentzian model for $\langle|h(q)|^2\rangle$ [22]

$$\langle|h(q)|^2\rangle = \frac{A \quad \sigma^2\xi^2}{(2\pi)^5(1 + aq^2\xi^2)^{1+H}} \tag{6}$$

with $a = (1/2H)[1 - (1 + aQ_c^2\xi^2)^{-H}](0 < H < 1)$ and $a = 1/2\ln(1 + aQ_c^2\xi^2)(H = 0)$. $Q_c = \pi/c$ with c a lower length scale cut-off of the order of the atomic spacing.

3.2. Mound roughness

Although noise-induced roughening can lead to the formation of self-affine fractal morphologies [12–15], such a growth does not always occur and instead the growth front can be rough in the sense that multilayer step structures are formed during growth [8–11]. In the former case the existence of an asymmetric step–edge diffusion barrier, or Schwoebel barrier, inhibits the down-hill diffusion of incoming atoms leading effectively to the creation of large structures in the form of mounds (corresponding to a roughness exponent $H = 1$) [8–11]. Mound rough morphologies have been described in the past by the interface roughness amplitude σ, the system correlation length ζ, which determines how randomly the mounds are distributed on the surface, and the average mound separation λ [22–26]. Such a rough morphology can be described by:

$$\langle|h(q)|^2\rangle = \frac{A \quad \sigma^2\zeta^2}{(2\pi)^5 \quad 2} e^{-(4\pi^2 + q^2\lambda^2)(\zeta^2/4\lambda^2)} I_0(\pi q\zeta^2/\lambda) \tag{7}$$

with $I_0(x)$ the modified (hyperbolic) Bessel function of the first kind and zero order. Note that for $\zeta \geq \lambda$ (strong Schwoebel barrier effect) a characteristic satellite ring at $q = 2\pi/\lambda$ of the power spectrum $\langle|h(q)|^2\rangle$ occurs.

4. RESULTS AND DISCUSSION

4.1. Self-affine roughness

From equation (6) we can derive an analytical form for ρ and thus for the force ratio. In fact, we have [27]

$$F_m/F \approx 1 - \frac{1}{2}\rho^2 + \frac{9}{8}\rho^4,\ \rho = \left[\frac{\sigma^2}{2a^2\xi^2}\left\{\frac{1}{1-H}[(1 + aQ_c^2\xi^2)^{1-H} - 1] - 2a\right\}\right]^{1/2}. \tag{8}$$

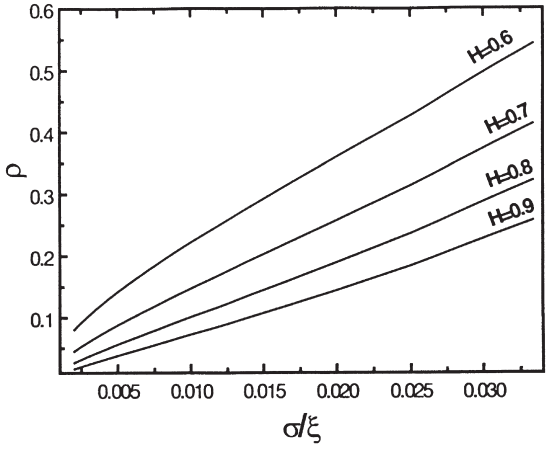

Fig. 2. Local slope for self-affine fractal roughness vs the long wavelength ratio σ/ξ for roughness exponents as indicated, $\sigma = 1$ nm and $c = 0.3$ nm.

Prior to the presentation of the results, we point out the following. The ratio σ/ξ describes mainly the long-wavelength ($q \ll 1/\xi$) roughness characteristics. Finer roughness details at short-wavelengths ($q \gg 1/\xi$) are revealed through the effect of the roughness exponent H. The latter describes the degree of height–height fluctuation irregularity and density, and it is related to a local fractal dimension $D = 3 - H$ [22]. In our calculations, we used for the roughness amplitude the value $\sigma = 1$ nm and correlation lengths ξ such that $\sigma/\xi \leq 0.1$ and c is taken to be equal to 0.3 nm. In order to illustrate the sensitivity of ρ on the roughness exponent H, Fig. 2 shows the variation of ρ versus the ratio σ/ξ for various adjacent roughness exponents H.

Fig. 3 displays the results of the calculations of the roughness effect on the measured stress force in the weak roughness limit for adjacent roughness exponents $H > 0.5$ and long wavelength ratios $\sigma/\xi < 0.1$. For roughness exponents $H < 0.5$ the weak roughness limit is achieved for a lower ratio of

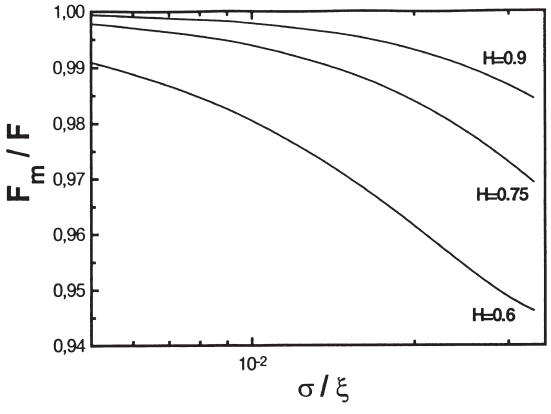

Fig. 3. Ratio between the measured to actual force vs the long wavelength ratio σ/ξ for roughness exponents as indicated, $\sigma = 1$ nm and $c = 0.3$ nm.

σ/ξ. Clearly with increasing ratio σ/ξ (or the long wavelength roughness) the force ratio decreases, the more so for decreasing roughness exponent H which leads to rougher interfaces at shorter roughness wavelengths. Therefore, for interfaces possessing this type of roughness, as observed in a wide range of surface interface studies by X-ray reflectivity and scanning probe microscopy [12–15, 18–21], the precise quantification of interface morphology is required to estimate properly the effect of roughness on the stresses in the thin film.

4.2. Mound roughness

Calculations were performed for mound roughness with $\sigma = 1$ nm and roughness parameters λ and ζ such that $\rho < 1$, see Fig. 4. The oscillatory behavior of ρ for $\lambda < \zeta$ originates effectively from the presence of a ring structure on the power spectrum leading for the corresponding real space height correlation function to oscillations at large lateral length scales. Clearly for small ζ (weak Schwoebel barrier) the behavior of the local slope is similar to that of the self-affine depicted in Fig. 2. The oscillatory behavior is reproduced in Fig. 5 which shows the roughness effect on the force ratio. While for $\zeta = 10$ nm a monotonic decay is observed with increasing ratio σ/λ in a manner similar to that of a self-affine roughness, an oscillatory behavior is found for $\zeta = 30$ and 60 nm, respectively. It indicates that a precise knowledge of the interface morphology is required to gauge properly the contribution of the roughness to the interfacial stress state.

It is interesting to note that even for a mound rough morphology an analytical expression can be obtained in the limit of very small values of the cut-off c in Q_c. Substitution of equation (7) into equation (5) leads to:

$$\rho = \left[A \frac{\Gamma(2)}{\mathrm{i}CB^{3/2}\Gamma(1)} M_{3/2,0}\left(-\frac{C^2}{4B}\right) \exp\left(\frac{C^2}{8B}\right)\right]^{1/2} \quad (9)$$

where $M_{\alpha,\beta}(z)$ is the Whittaker function and

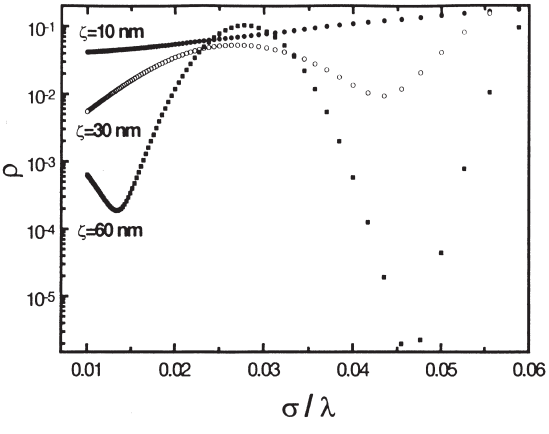

Fig. 4. Local slope for mound roughness vs the long wavelength ratio σ/λ for system correlation lengths ζ as indicated, $\sigma = 1$ nm and $c = 0.3$ nm.

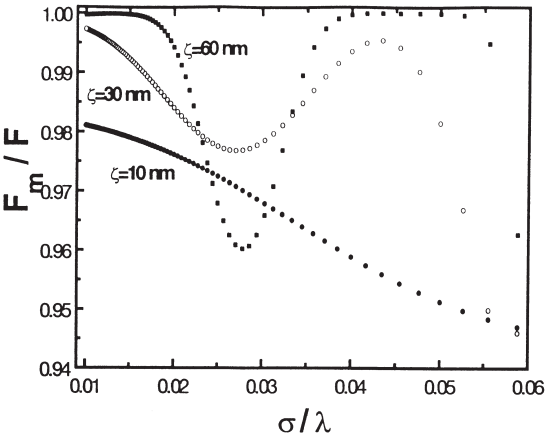

Fig. 5. Ratio between the measured to actual force vs the long wavelength ratio σ/λ for system correlation lengths ζ as indicated, $\sigma = 1$ nm and $c = 0.3$ nm.

$A = 2B\sigma^2\exp(-C^2/4B)$, $B = \zeta^2/4$, $C = \pi\zeta^2/\lambda$. By using the mathematical relationship between $M_{\alpha,\beta}(z)$ and the confluent hypergeometric function, equation (9) can be written in the limit of very small lower length-scale cut-off c simply by:

$$\rho = \frac{2\sigma}{\zeta}\sqrt{1 + \frac{\pi^2\zeta^2}{\lambda^2}} \quad (10)$$

4.3. General expression for F_m/F

In both cases of the roughness the calculations of the force ratio F_m/F were performed for local slopes $\rho < 0.5$ within the second order of the perturbation expansion. For higher values of the local slope (but still $\rho < 1$) additional terms have to be incorporated in equation (5). A more general expression for the force ratio reads:

$$F_m/F = 1 + \sum_{n=1}^{+\infty} \frac{(-1/2)(-1/2-1)\ldots(-1/2-n+1)}{n!} \int \langle(\nabla h)^{2n}\rangle d^2r \quad (11)$$

which after substitution from equation (A.8) changes into

$$F_m/F = 1 + \sum_{n=1}^{+\infty} \frac{(-1/2)(-1/2-1)\ldots(-1/2-n+1)}{n!} P(n)\rho^{2n} \quad (12)$$

with, i.e. $P(1) = 1$ and $P(2) = 3$. Indeed, $P(n)$ represents all possible ways to group $2n - h(q)s$ during ensemble average in pairs of two [28].

5. CONCLUSIONS

In order to investigate the effect of roughness parameters on measurement of the force, we combine the knowledge of interface stress theory related to roughness with analytic descriptions of the height–height correlations for self-affine and mound rough interfaces. Although our calculations are performed in the weak roughness limit (which corresponds to low roughness contribution), the results indicate that the roughness morphology may affect the measurement of interface stress and a method has been developed to incorporate the necessary corrections if precise roughness data are available.

Acknowledgements—The authors are grateful to Professor Frans Spaepen for his comments on an earlier version of this paper. We would like to acknowledge support from the Netherlands Institute for Metals Research, and the "Stichting voor Fundamenteel Onderzoek der Materie" (FOM-Utrecht) which is financially supported by the Nederlandse Organisatie voor Wetenschappelijk Onderzoek (NWO-The Hague).

Appendix A

The assumption that $h(r)$ is a Gaussian variable means that the average of any odd number of factors of $h(r)$ with the same or different arguments vanishes, whereas the average of the product of an even number of factors of $h(r)$ is given by the sum of the products of the averages of the $h(r)$s paired two-by-two in all possible ways, i.e. we have [29]

$$\begin{aligned}&\langle h(r)h(r')h(r'')h(r''')\rangle = \\ &\langle h(r)h(r')\rangle\langle h(r'')h(r''')\rangle + \\ &\langle h(r)h(r'')\rangle\langle h(r')h(r''')\rangle + \\ &\langle h(r)h(r''')\rangle\langle h(r')h(r'')\rangle\end{aligned} \tag{A.1}$$

Fourier transformation of equation (A.1) yields

$$\begin{aligned}&\langle h(q)h(q')h(q'')h(q''')\rangle = \\ &\langle h(q)h(q')\rangle\langle h(q'')h(q''')\rangle + \\ &\langle h(q)h(q'')\rangle\langle h(q')h(q''')\rangle + \\ &\langle h(q)h(q''')\rangle\langle h(q')h(q'')\rangle\end{aligned} \tag{A.2}$$

where each pair in equation (A.2) can be calculated according to:

$$\begin{aligned}&i^{2n}\int\left\langle \prod_{j=1}^{2n} h(q_j)\right\rangle \prod_{j=1}^{2n} q_j e \\ &\quad{}^{-i\left(\sum_{j=1}^{2n} q_j\right)r}\prod_{j=1}^{2n} d^2q_j = \\ &P(n)\rho^{2n}\end{aligned} \tag{A.3}$$

will appear with $i^{2n} = (-1)^n$. Thus, the integrals in equation (A.3) for $n = 1,2$ will be given by

$$\begin{aligned}&-\int\langle h(q_1)h(q_2)\rangle(q_1\cdot q_2)e^{-i(q_1+q_2)r}d^2q_1d^2q_2 \\ &=\langle(\nabla h)^2\rangle = \rho^2;\end{aligned} \tag{A.4}$$

$$\begin{aligned}&\int\left\langle \prod_{j=1}^{4} h(q_j)\right\rangle\left(\prod_{j=1}^{4} q_j\right)e^{-i\left(\sum_{j=1}^{4} q_j\right)r}\prod_{j=1}^{4} d^2q_j = \\ &3\left\langle(\nabla h)^4\right\rangle = 3\rho^4.\end{aligned} \tag{A.5}$$

For higher order terms further concepts of statistics are needed to calculate $P(n)$ which represents all possible ways to group $2n - h(q)$s ensemble averaged in pairs of two [28].

REFERENCES

1. Tsao, J. Y., *Materials Fundamentals of Molecular Beam Epitaxy*. Academic Press, San Diego, 1993.
2. De Hosson, J. Th. M., Groen, H. B., Kooi, B. J. and Vitek, V., *Acta mater.*, 1999, **47**, 4077–4093.
3. Chaudhari, P., *J. Vac. Sci. Technol.*, 1972, **9**, 520.
4. Finegan, J. D. and Hofman, R. W., *J. Appl. Phys.*, 1959, **30**, 185.
5. Hofman, R. W., *Thin Solid Films*, 1985, **34**, 185.
6. Hofman, R. W., *Surf. Interface Analysis*, 1981, **3**, 62.
7. Spaepen, F., *Acta mater.*, 2000, **48**, 31.
8. Halpin-Healy, T. and Zhang, Y. -C., *Phys. Rep.*, 1995, **254**, 215.
9. Villain, J., *J. Phys. I (France)*, 1991, **1**, 19.
10. Johnson, M. D., Orme, C., Hunt, A. W., Graff, D., Sudijono, J., Sander, L. M. and Orr, B. G., *Phys. Rev. Lett.*, 1994, **72**, 116.
11. Siegert, M. and Plischke, M., *Phys. Rev. Lett.*, 1994, **73**, 1517.
12. Meakin, P., *Phys. Rep.*, 1994, **235**, 1991.
13. Krim, J. and Palasantzas, G., *Int. J. Mod. Phys. B*, 1995, **9**, 599.
14. Peitgen, H. -O., Jürgens, H. and Saupe, D., *Chaos and Fractals*. Springer-Verlag, New-York, 1992.
15. Meakin, P., *Fractals, Scaling and Growth Far From Equilibrium*. Cambridge University Press, Cambridge, 1998.
16. Aué, J. and De Hosson, J. Th. M., *Appl. Phys. Lett.*, 1997, **71**, 1347–1349.
17. Agterveld, D. T. L., Palasantzas, G. and De Hosson, J. Th. M., *Appl. Phys. Lett.*, 1999, **75**, 1080–1082.
18. Paniago, R., Forest, R., Chow, P. C., Moss, S. C., Parkin, S. P. and Cookson, D., *Phys. Rev. B*, 1997, **56**, 13442.
19. Sinha, S. K., Sirota, E. B., Garoff, S. and Stanley, H. B., *Phys. Rev. B*, 1988, **38**, 2297.
20. Holy, V., Kubena, J., Ohlidal, I., Lischka, K. and Plotz, W., *Phys. Rev. B*, 1993, **47**, 15896.
21. Chladek, M., Volvoda, V., Dorner, C., Holy, C. and Grim, J., *Appl. Phys. Lett.*, 1996, **69**, 1318.
22. Zhao, Y. -P., Yang, H. -N., Wang, G. -C. and Lu, T. -M., *Phys. Rev. B*, 1998, **57**, 1922.
23. Mandelbrodt, B. B., *The Fractal Geometry of Nature*. Freeman, New York, 1982.
24. Family, F. and Viscek, T., *Dynamics of Fractal Surfaces*. World Scientific, Singapore, 1991.
25. Palasantzas, G., *Phys. Rev. B*, 1993, **48**, 14472.
26. Palasantzas, G., *Phys. Rev. B*, 1994, **49**, 5785.
27. Palasantzas, G., *Phys. Rev. E*, 1997, **56**, 1254.
28. Spiegel, M. R., *Probability and Statistics* (Schaum's Outline Series), 1975
29. Farias, G. A. and Maradudin, A. A., *Phys. Rev. B*, 1983, **28**, 5675.